

# **Progress Towards Superconductor Electronics Fabrication Process with Planarized NbN Layers**

**Sergey K. Tolpygo, Justin Mallek, Vladimir Bolkhovsky, Ravi Rastogi, Evan B. Golden, Terence J. Weir, Leonard M. Johnson, and Mark A. Gouker**

**24 October 2022**



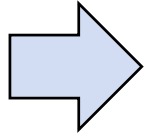
**This material is based upon work supported by the Under Secretary of Defense for Research and Engineering under Air Force Contract No. FA8702-15-D-0001. Any opinions, findings, conclusions or recommendations expressed in this material are those of the authors and do not necessarily reflect the views of the Under Secretary of Defense for Research and Engineering**



# Outline

“All intelligent thoughts have already been thought; what is necessary is only to try to think them again”

Johann Wolfgang von Goethe

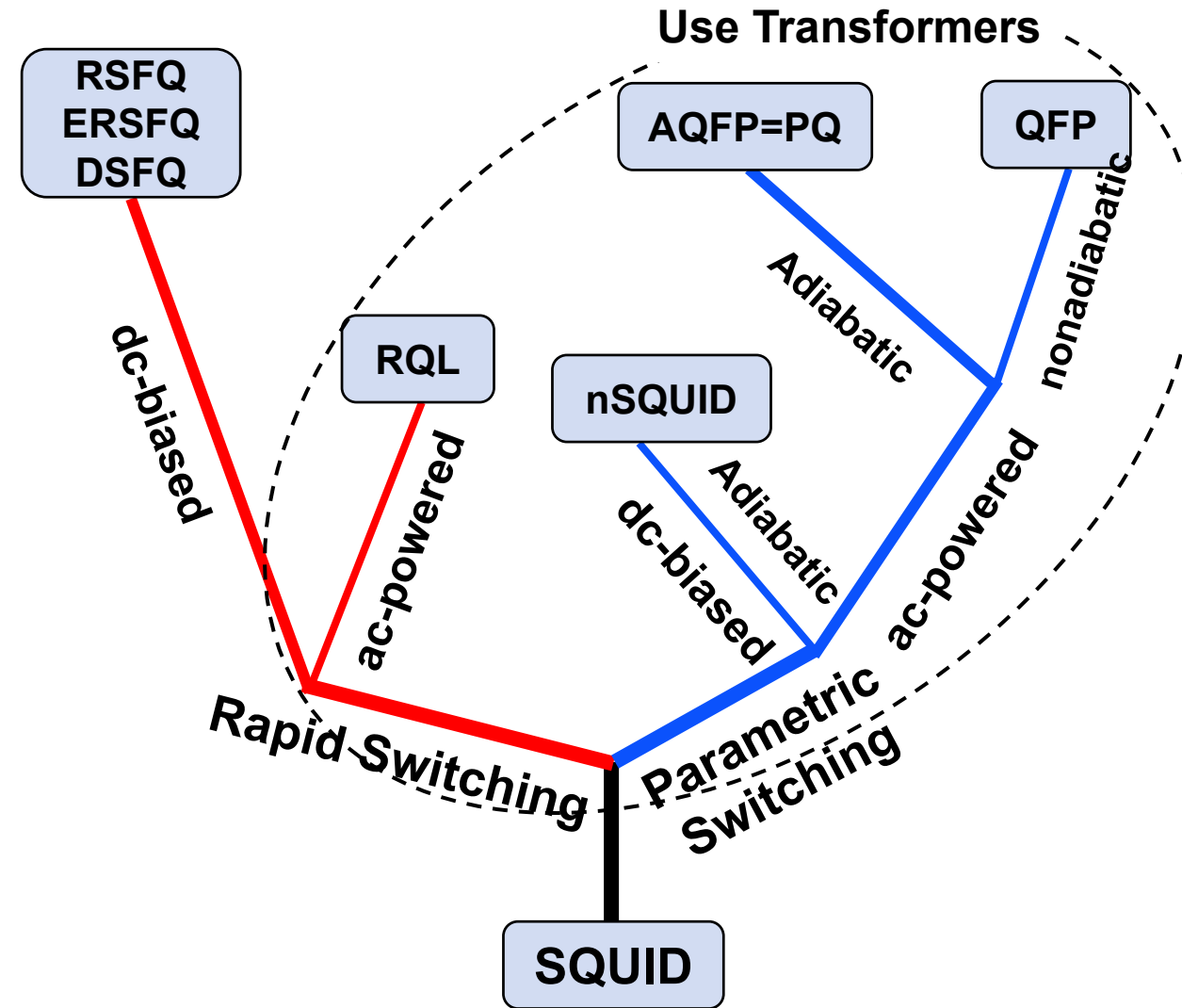


- Introduction
- Motivation: why we want NbN layers in the process stack
- Properties of NbN films
  - Critical currents of lines and vias
  - 1-NbN + 7-Nb-layer process SFQ5e++
  - Inductance and mutual inductance of NbN inductors in the 9-metal-layer process ([poster 1EPo2A-8 today](#))
- Why we do not want all NbN layers in the process stack
- Reconciliation of the requirements: Bilayer NbN/Nb inductors; [see also Invited poster 2EPo2F-1 on Tuesday, 2:15 pm – 4:15 pm](#)
- Conclusion



# Tree of Superconductor Digital Electronics

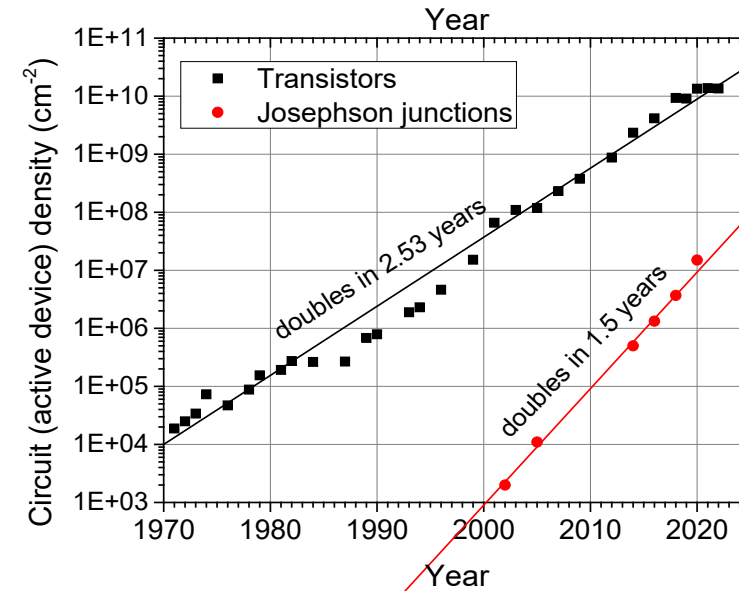
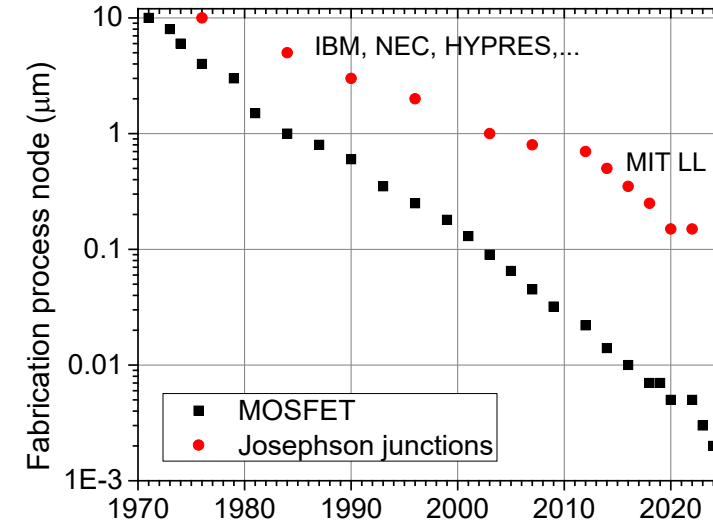
- **SQUID** – superconducting quantum interference device
  - dc SQUID – dc current, two-junction quantum interferometer (1964)
  - rf SQUID – single-junction quantum interferometer using rf excitation (1965)
- **PQ** – Parametric Quantron (1976)
- **QFP** – Quantum Flux Parametron (1985)
- **RSFQ** – Rapid Single Flux Quantum (1985)
- **nSQUID** – negative inductance SQUID (2003)
- **RQL** – Reciprocal Quantum Logic (2011)
- **ERSFQ** – Energy-efficient RSFQ (2011)
- **AQFP** – Adiabatic QFP (2012)
- **DSFQ** – Dynamic SFQ (2018)





# Introduction

- **Superconductor electronics (SCE) has demonstrated**
  - The highest clock rates (up to  $\sim 750$  GHz in simple devices and  $\sim 140$  GHz in relatively complex circuits)
  - The lowest energy dissipation (down to  $\sim 5k_B T$  per bit )
- **Main problem – low circuit (device) density and integration scale (device count) of SCE, resulting in low functionality**
  - 150 nm process node at LL vs 3 nm CMOS at TSMC
  - 1000x lower circuit density of SCE than in CMOS
- **Example: IARPA Supertools Program SFQ cell library**
  - The maximum (E)RSFQ circuit density is  $5 \cdot 10^5$  JJs/cm<sup>2</sup>
  - The maximum AQFP circuit density is  $4.6 \cdot 10^5$  JJs/cm<sup>2</sup> ( $1.6 \cdot 10^5$  JJs/cm<sup>2</sup> in AIST, Japan cell library)
  - These densities are almost 5 orders of magnitude lower than in CMOS





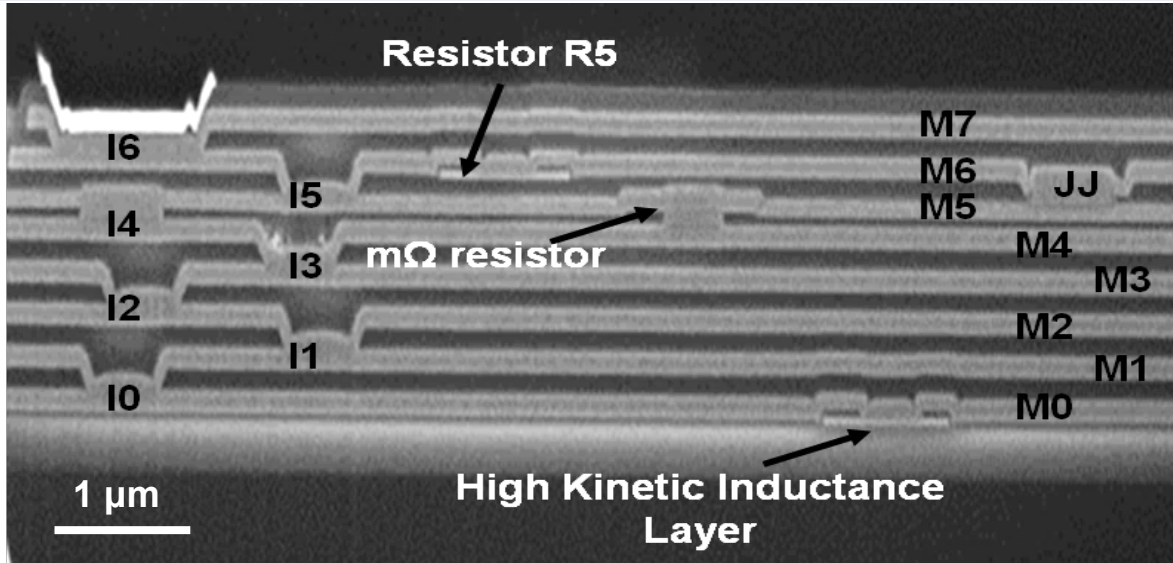
# Integration Scale Limiters

- **The main cause of disparity between SCE and CMOS in integration scale is in information encoding**
  - In CMOS, information encoded by a presence/absence of a static charge (voltage) on a capacitor
  - In SCE, information encoded by a presence /absence of circulating current (magnetic flux) in a superconducting loop, i.e. by moving charges
  - Obviously, moving charges always take more space than localized charge
- **Factors limiting integration scale are related to flux (information) manipulation:**
  - Minimal critical current of Josephson junctions (min area) is set by thermal fluctuations (bit errors)
  - Area occupied by superconducting inductors
  - Area occupied by ac excitation (clock) and flux bias transformers
  - Crosstalk between ac-driven power lines and logic cells
  - Critical current of superconducting wires and vias
- **Increasing integration scale requires technology solutions commensurate with benefits**
  - *E.g.*, do we ultimately need a 120-nm, or 65-nm, or 45 nm technology? (Certainly not 3-nm)
- **Materials limitations and fabrication challenges**

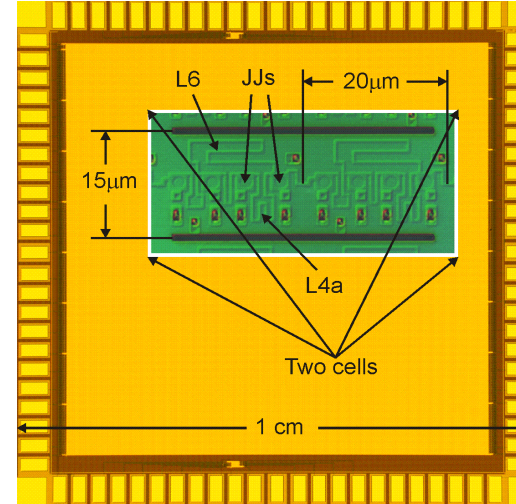




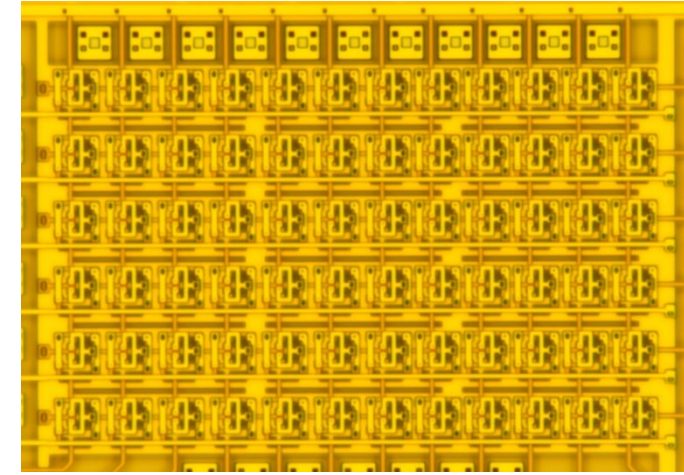
# MIT LL Standard Fabrication Node SFQ5ee



## 202 Kb Shift Register



## JJ RAM



### Process Features

- 200-mm wafer size
- Junctions: Nb/AIO<sub>x</sub>-Al/Nb;  $J_c = 0.1$  and  $0.2 \text{ mA}/\mu\text{m}^2$
- Min JJ size: 600 nm
- Superconducting layers: 9
  - 8 niobium wiring layers
  - 1 layer of Mo<sub>2</sub>N (kinetic inductors for biasing)
  - Resistors:  $2 \text{ } \Omega/\text{sq}$  or  $6 \text{ } \Omega/\text{sq}$ ;  $\text{m}\Omega$  resistor is N/A
- Min inductor linewidth: 350 nm

- AC-biased shift register: 202,280 bits
- 809,120 shunted  $1.25\text{-}\mu\text{m}^2$  JJs
- Over 4 million inductors
- Circuit density:  $1.33\text{M JJs}/\text{cm}^2$
- Integration scale:  $\approx$  Intel's Pentium II,  $0.8\text{-}\mu\text{m}$  process,  $3.1\text{M}$  transistors on  $294 \text{ mm}^2$  chip in 1993

V.K. Semenov, Y.A. Polyakov, and S.K. Tolpygo, *IEEE Trans. Appl. Supercond.*, vol. 27, no. 4, 1301409, June 2017

- Array pitch:  $9 \text{ } \mu\text{m} \times 12 \text{ } \mu\text{m}$
- Circuits density:  $3.7 \times 10^6 \text{ JJ}/\text{cm}^2$  record density for SCE
- Functional density:  $1 \text{ Mb}/\text{cm}^2$
- Technology: self-shunted JJs,  $w = 0.4 \text{ } \mu\text{m}$   
 $J_c = 0.6 \text{ mA}/\mu\text{m}^2$

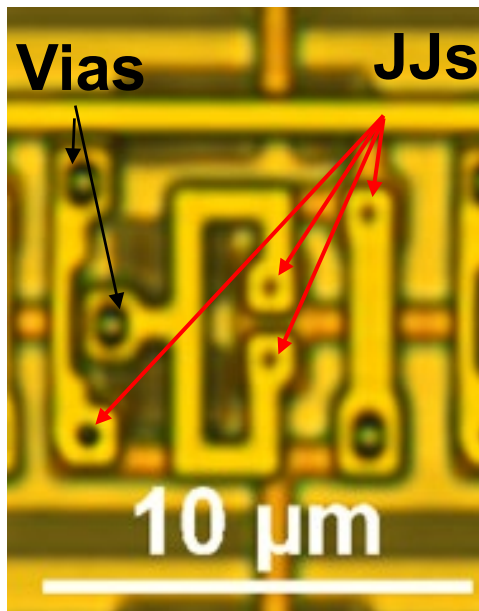
V.K. Semenov, Y.A. Polyakov, and S.K. Tolpygo, *IEEE Trans. Appl. Supercond.*, vol. 29, no. 5, 1302809, Aug. 2019



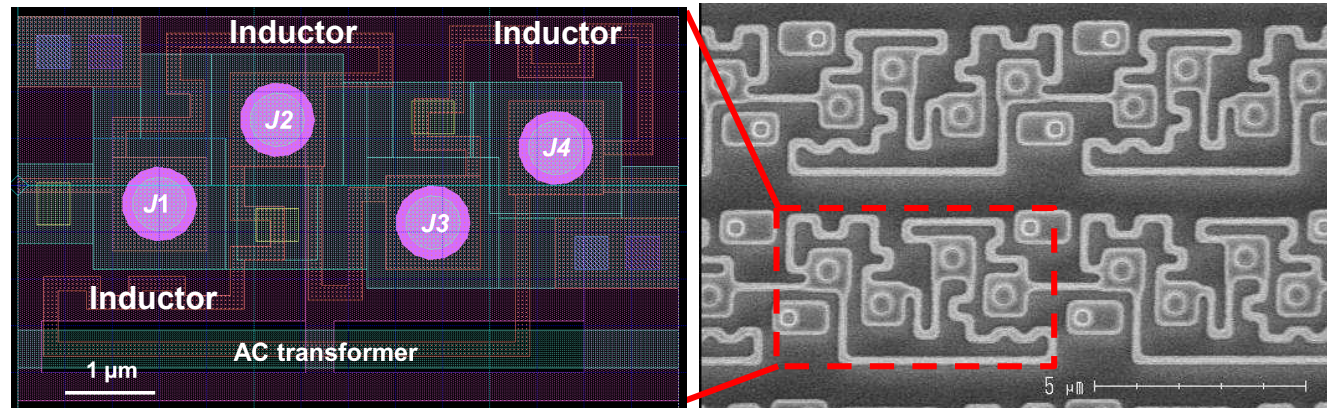
# Density of Circuits With Self-Shunted Junctions

- $J_c = 600 \mu\text{A}/\mu\text{m}^2$
- AC-clocked shift registers
  - Cell dimensions:  $7 \mu\text{m} \times 4 \mu\text{m}$
  - Circuit density:  $1.3 \cdot 10^7 \text{ JJ}/\text{cm}^2$
  - 150-nm linewidth
  - 2x increase over the 250-nm process

### JJ RAM Cell



### Shift Register, 150-nm linewidth



Most of the circuit area is occupied by inductors and transformers, <11% by Josephson junctions

Circuit Components in RAM (Shift Register) Cell	Occupied Area (%)
NDRO transformer wires, 0.4 μm linewidth	7.2
Write/Read transformer wires	5.4
Perforations in transformers ground planes for increasing mutual inductance	23 (11)
Flux trapping moats	4 (6)
Josephson junctions	3.5 (11)
Interlayer vias	3 (13)





# Balancing Densities of Inductors and Junctions

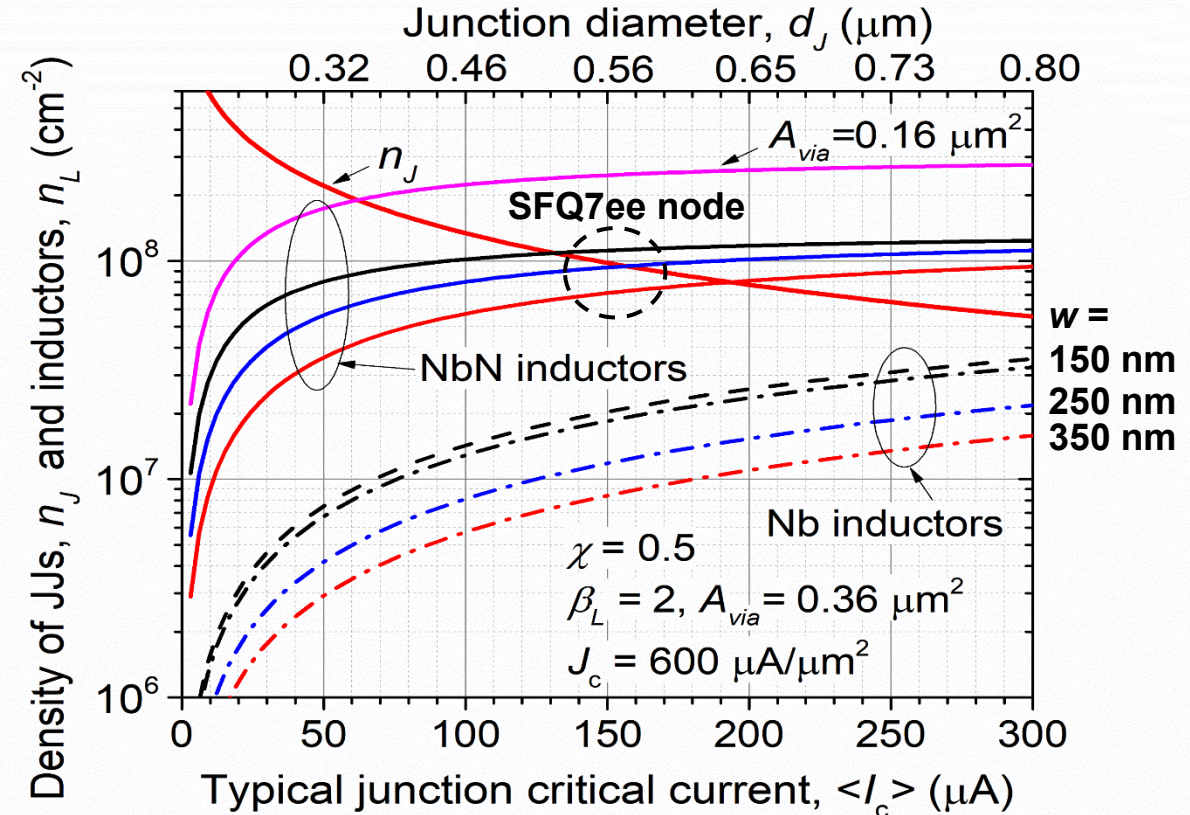
- At  $J_c \sim 600 \mu\text{A}/\mu\text{m}^2$ , Nb/Al-AIO<sub>x</sub>/Nb junctions are self-shunted and do not require shunt resistors; JJ density:

$$n_J = \chi \left( \left( \frac{4\langle I_c \rangle}{\pi J_c} \right)^2 + \delta \right)^{-2} \quad (1)$$

- $\chi$  – fill-factor,  $\langle I_c \rangle$  - critical current of JJs,  $\delta$  – junction surround
- Density of inductors:

$$n_L = \chi \left( \frac{\beta_L \Phi_0}{2\pi \langle I_c \rangle L_L} (w + s) + A_{via} \right)^{-1} \quad (2)$$

- Densities of JJs and inductors need to be balanced: one JJ requires one inductor on average
- With Nb inductors, circuits are “starved”: not enough inductors
- NbN kinetic inductors allow us to achieve 100 million devices per cm<sup>2</sup> (10x increase)
- $I_c \sim 50 \mu\text{A}$  requires  $d \approx 0.3 \mu\text{m}$  – the next challenge



Solid curves: NbN stripline inductors with  $w = 250 \text{ nm}$  and thickness, from bottom to top,  $200 \text{ nm}$ ,  $100 \text{ nm}$ , and  $50 \text{ nm}$ . The uppermost solid magenta curve corresponds to NbN striplines with  $w = 150 \text{ nm}$ ,  $t = 50 \text{ nm}$ , and  $A_{via} = 0.16 \mu\text{m}^2$  in (2)





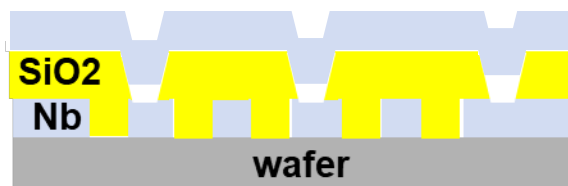
# Motivation for Using NbN and Technical Goals

- Increasing integration scale of SCE by 10x:
  - Reduce area of inductor – need 10x higher inductance per unit length than Nb inductors
  - Decrease min linewidth and spacing of superconducting wires
  - Decrease size of interlayer vias (350 nm now)
- Requires replacement of Nb by ? and development of damascene processing of superconducting materials
- Energy efficiency advantage of SCE over CMOS reaches ~100x if operating temperature of SCE is increased to ~10 K (may not be achievable)
  - Requires implementation of higher- $T_c$  materials, e.g., NbN and NbTiN in the layer stack
    - Conformal thin film deposition
    - High-density plasma etching
    - Chemical mechanical planarization (CMP)

How processing is done now:



Nb deposition and patterning



Via etch and Nb deposition



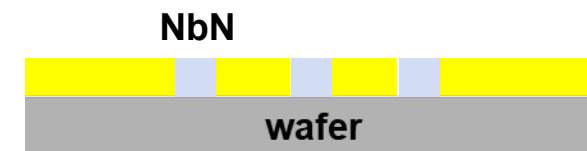
SiO<sub>2</sub> deposition and CMP

Narrow gaps between Nb wires cannot be filled by SiO<sub>2</sub> and high-aspect-ratio via cannot be filled by Nb deposition at low temp.

Our approach – replace Nb and use damascene processing



SiO<sub>2</sub> deposition and patterning trenches in dielectric

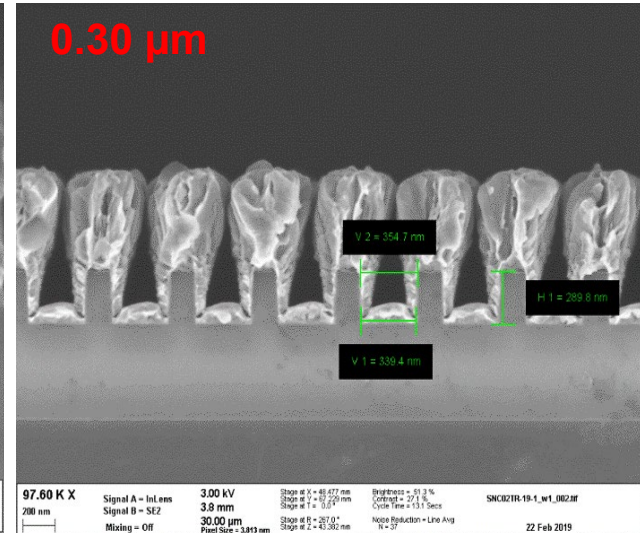
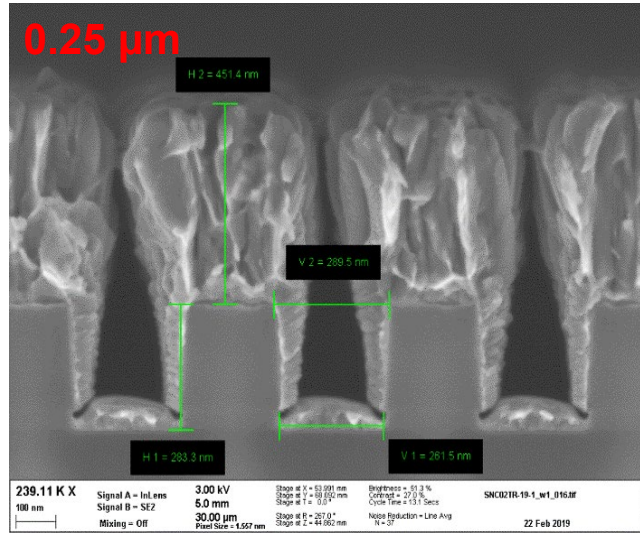


NbN or NbTiN conformal PECVD or PEALD and planarization using metal CMP

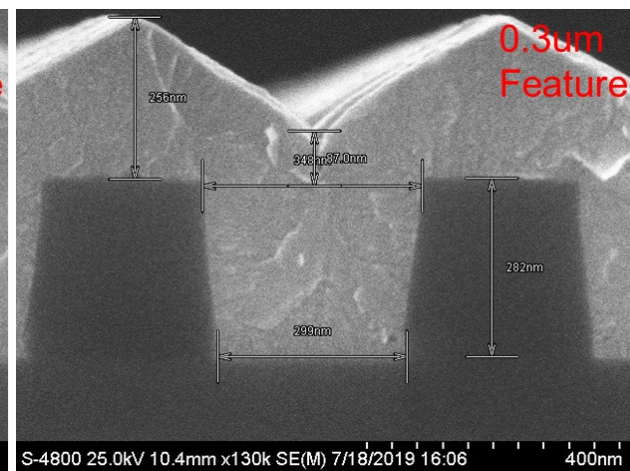
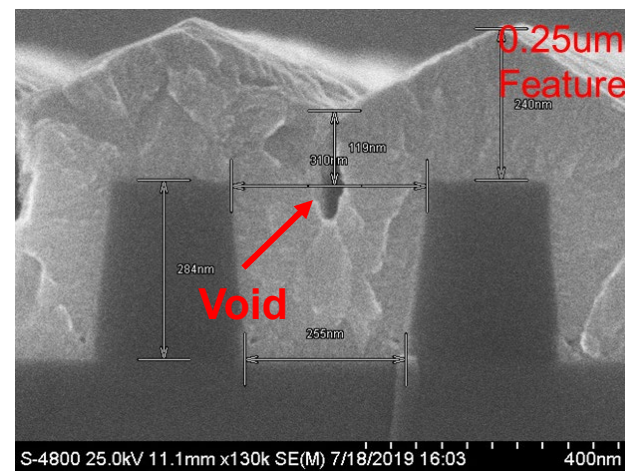


# (Not) Filling Narrow Trenches by PVD

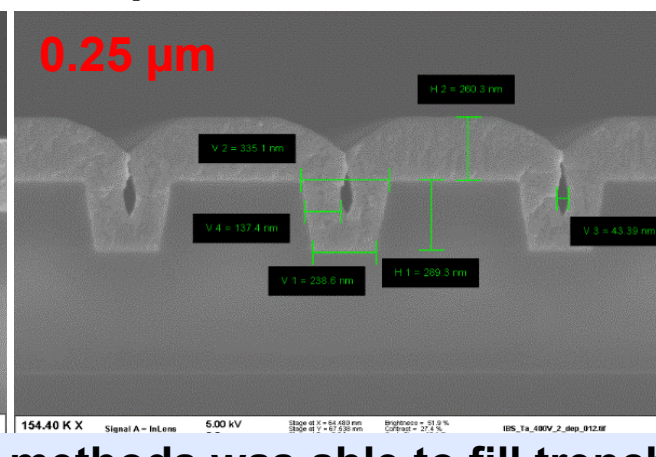
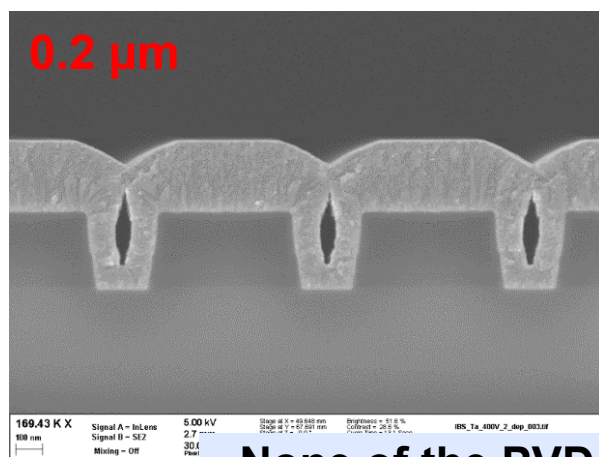
## Nb Sputtering in Endura AMAT



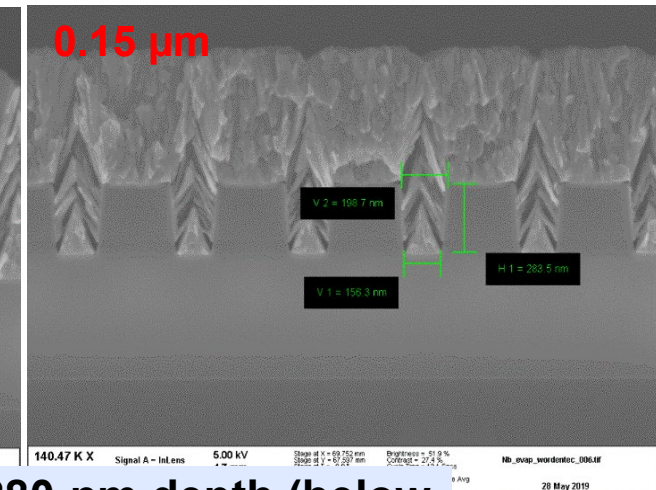
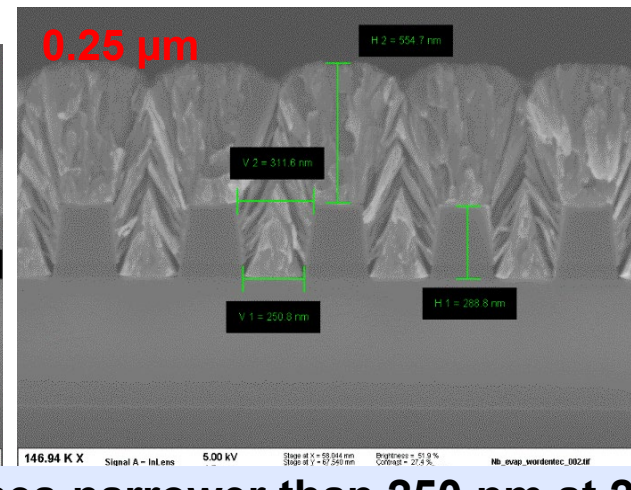
## Ionized Metal Plasma, SIP EnCoRe Process (AMAT)



## Ion Beam Assisted Deposition



## Nb E-beam Evaporation



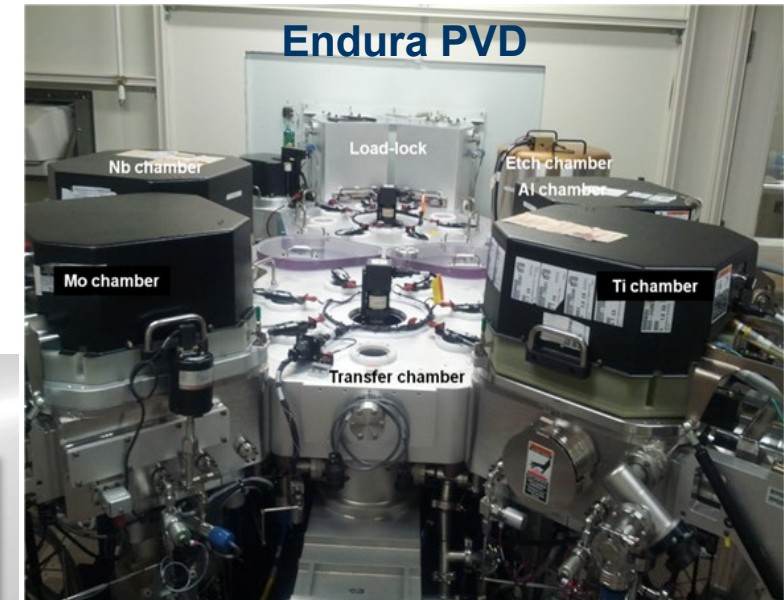
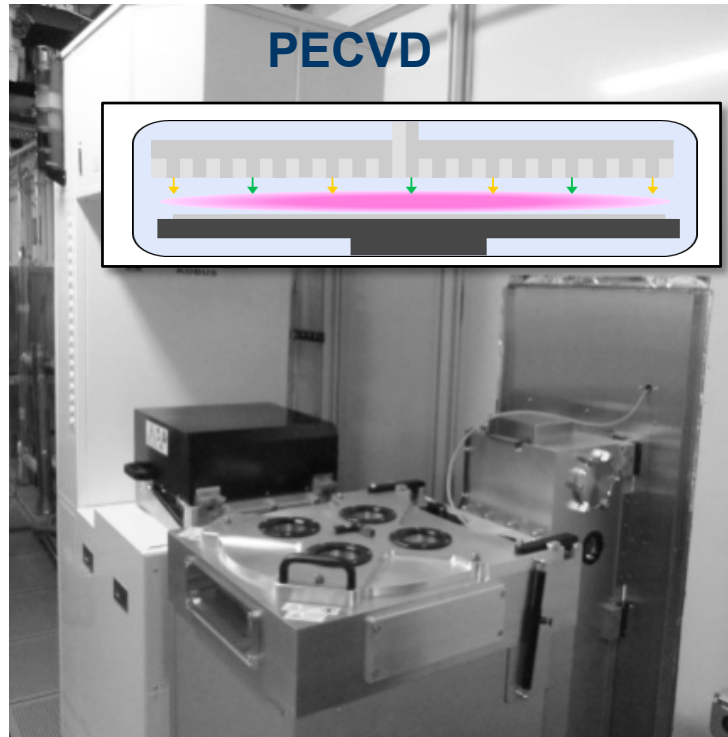
None of the PVD methods was able to fill trenches narrower than 250 nm at 280-nm depth (below 1:1.1 aspect ratio) with Nb at  $T < 200$  °C without voids and Nb degradation – need (PE)CVD





# NbN and NbTiN Deposition: PVD and PECVD/ALD

- **Reactive sputtering for NbN planar films and filling low aspect ratio via, not for damascene**
  - $N_2/Ar$  gas, Nb target, magnetron sputtering
  - Deposition temperature: 20 °C – 400 °C
- **Plasma-enhanced chemical vapor deposition (PECVD) for filling high aspect ratio structures and damascene processing**
  - Utilizes volatile metal-organic precursors to produce highly conformal thin films
  - Two on-board precursors for deposition of TiN, NbN, and NbTiN
  - $H_2$ ,  $N_2$ , and  $NH_3$  reactant gasses enable thermal and plasma-based deposition of high quality films
  - Uses high-frequency and low-frequency plasma, fast cycling valves and fast matching high frequency to enable ultra short deposition cycles





# Critical Current of Wires: NbN vs Nb

- Should be much larger than  $I_c$  of JJs,  $\gg 100 \mu\text{A}$
- Fundamental limit to the superconductor critical current density is

$$j_c^{GL} = \frac{2\sqrt{2}}{3\sqrt{3}} \frac{B_c}{\mu_0 \lambda},$$

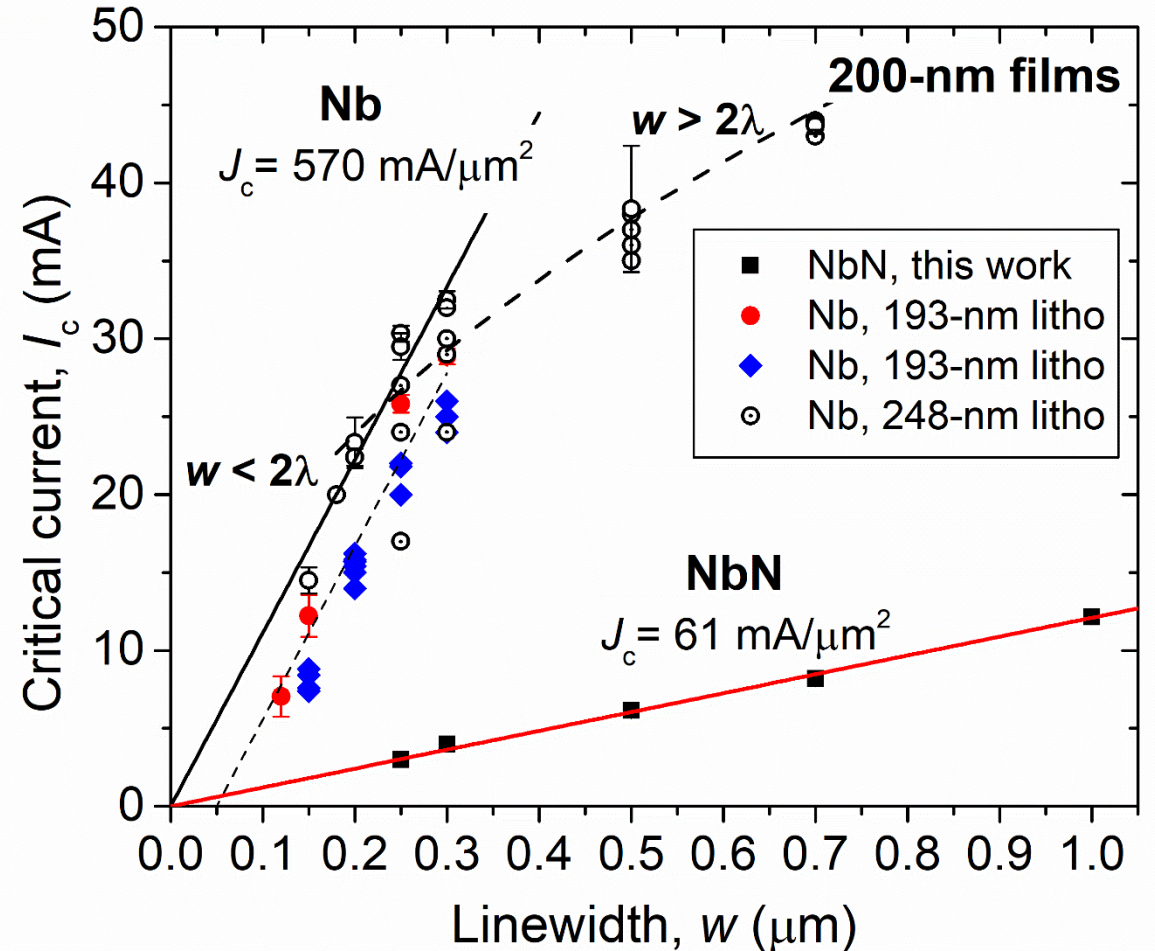
the so-called Ginzburg-Landau (pair-breaking) critical current;  $B_c$  - thermodynamic critical magnetic field,  $\lambda$  - penetration depth

- For Nb:  $B_c = 0.122 \text{ T}$  at 4.2 K,  $\lambda = 90 \text{ nm}$ , giving

$$j_c^{GL}(4.2 \text{ K}) = 0.59 \text{ A}/\mu\text{m}^2$$

- NbN:  $\lambda = 491 \text{ nm}$  is 5.5 $\times$  larger and  $j_c$  is about 9 times lower than in Nb films because of lower density of Cooper pairs and higher resistivity

Critical current of superconductors is inversely proportional to their kinetic inductance

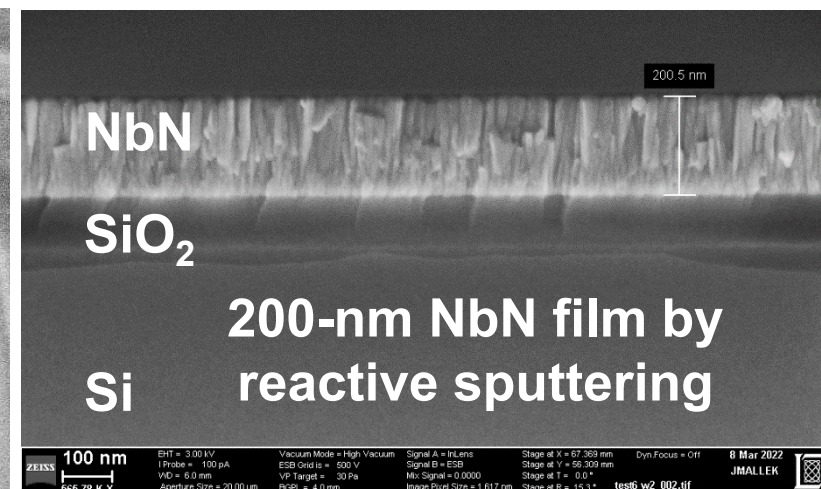
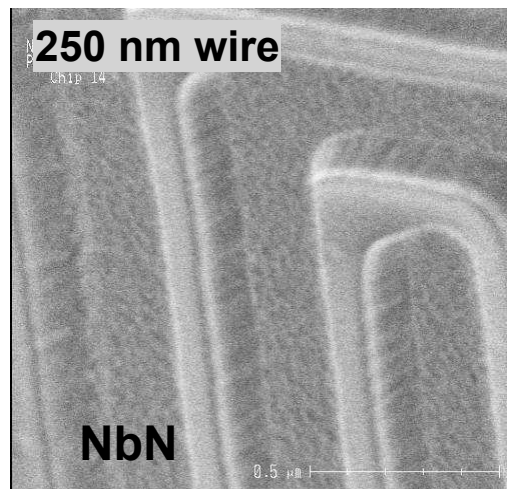






# Characterization of Reactively Sputtered NbN Films

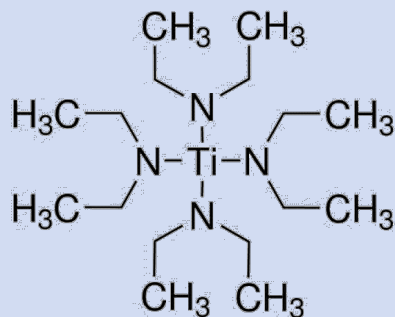
- $T_c$  of PVD NbN films is up to 16.5 K
- Demonstrated superconducting vias and hundreds of 1800-via chains between two NbN layers (M1 and M2) and between NbN and Nb layers
- Investigated stability of NbN films and patterned films imbedded in SiO<sub>2</sub> up to 400 °C:
  - Critical temperature,  $T_c$
  - Critical currents of patterned lines,  $I_c$
  - Critical current of NbN vias
- Only minor degradation of NbN film have been detected at high deposition temperatures of SiO<sub>2</sub> using TEOS or SiH<sub>4</sub> PECVD
  - Similar Nb structures *would not be superconducting under the same conditions*
- Residual stress in NbN films was adjusted to compressive ~ -300 MPa



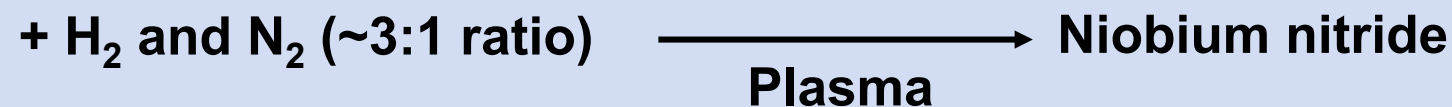
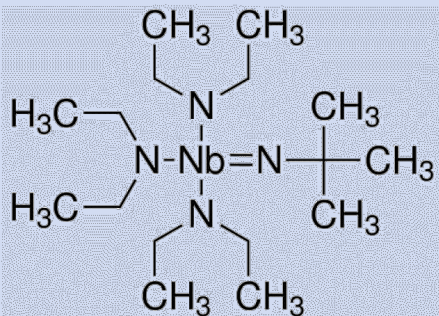
Parameter	SiO <sub>2</sub> deposition at 150 °C	SiO <sub>2</sub> deposition at 400 °C
$T_c$ (K)	15.9	15.5
$I_c$ of 0.7-μm wires (mA)	5.2	4.2
$I_c$ of 0.7-μm vias (mA)	7.0	6.1



# PECVD Process for TiN and NbN



**Tetrakis(diethylamino)titanium(IV)**  
**TDEAT**



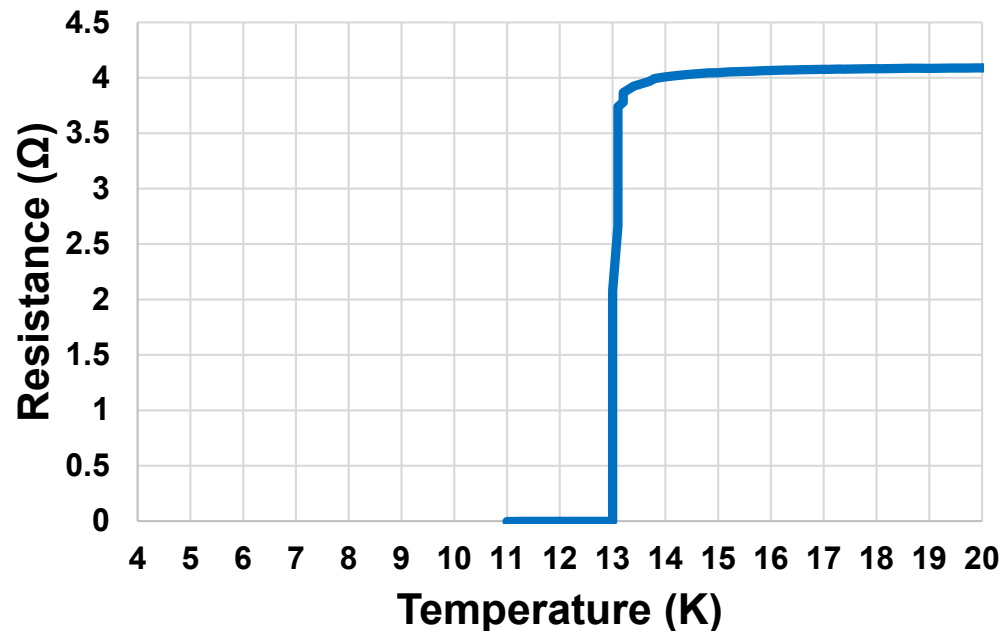
**Tris(diethylamido)(tert-butylimido)niobium(V)**  
**TBTDEN**

**Deposition temperature 150 °C – 400 °C**



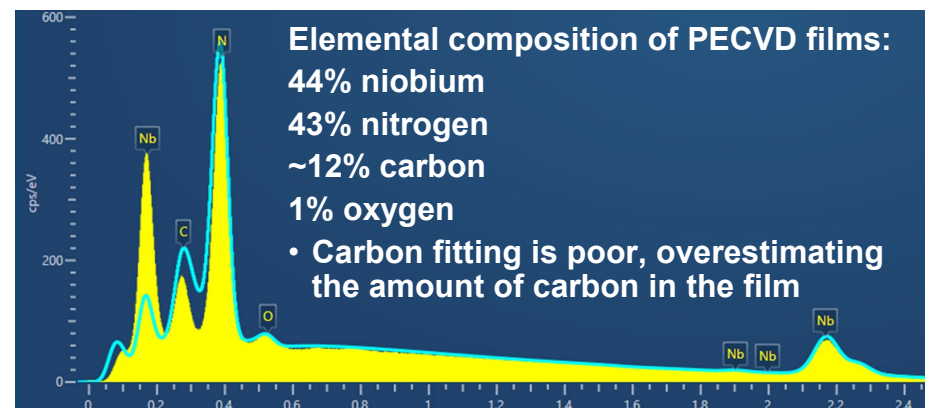
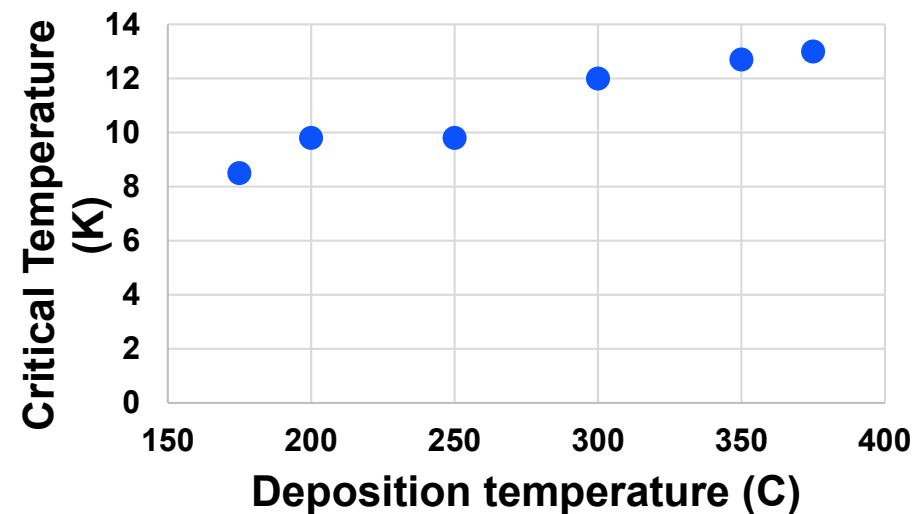
# Superconducting Properties of PECVD NbN Films

## Superconducting transition of PECV-deposited NbN film



- $T_c$  of up to 13 K has been obtained in PECVD NbN films
- Up to 16.5 K using reactive sputtering
- $R(T)$  dependence in the range from  $T_c$  to 300 K indicates good quality of PECVD NbN

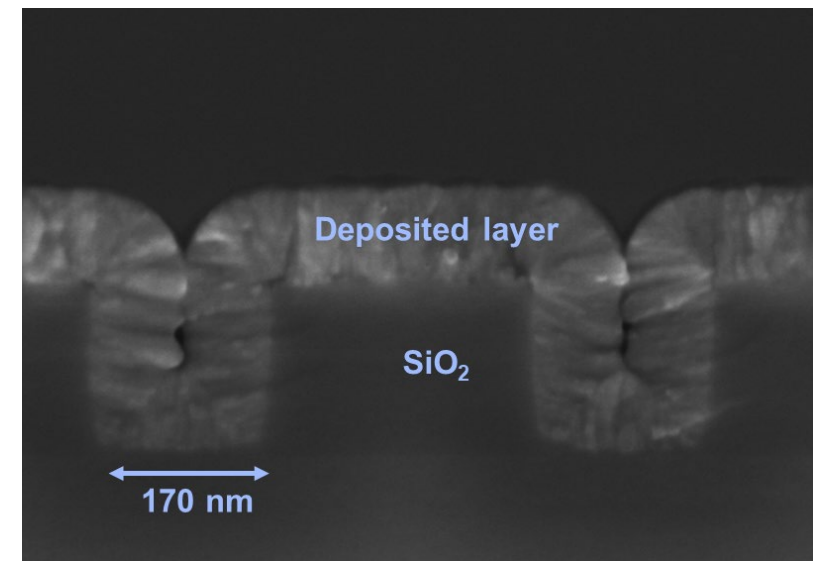
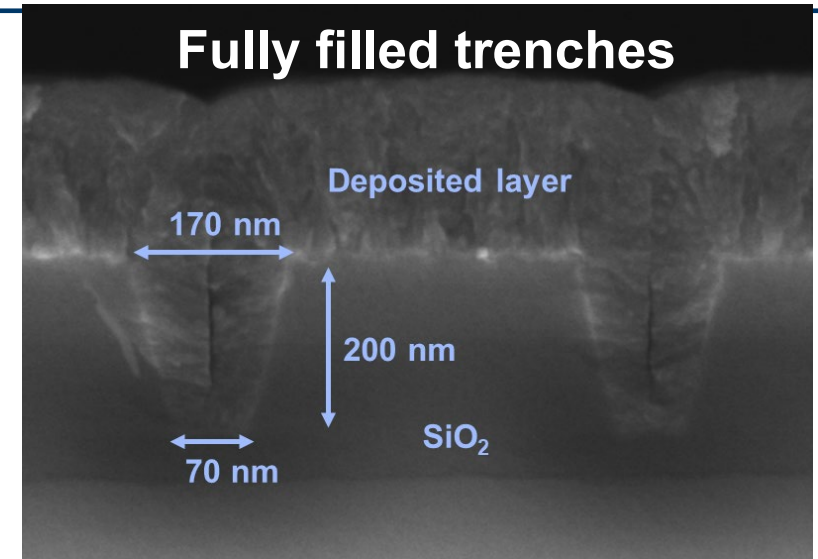
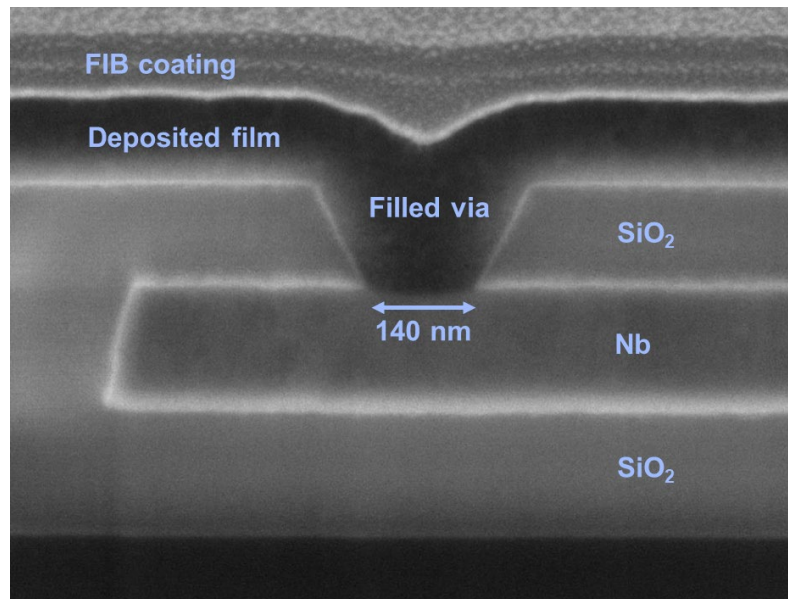
## Critical temperatures of PECVD NbN films





# Conformal PECVD of NbN in Narrow Trenches and Vias

- Developed highly conformal via fill for via size sizes below 200 nm, using sloped sidewalls
- Additional recipe development may lead to fully planarized films over filled via
- A planarized deposition process may eliminate the need for chemical mechanical planarization (CMP)
- Demonstrated filling narrow trenches with minimal seaming and nearly planar overgrowth using PECVD

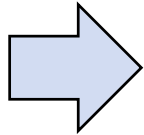






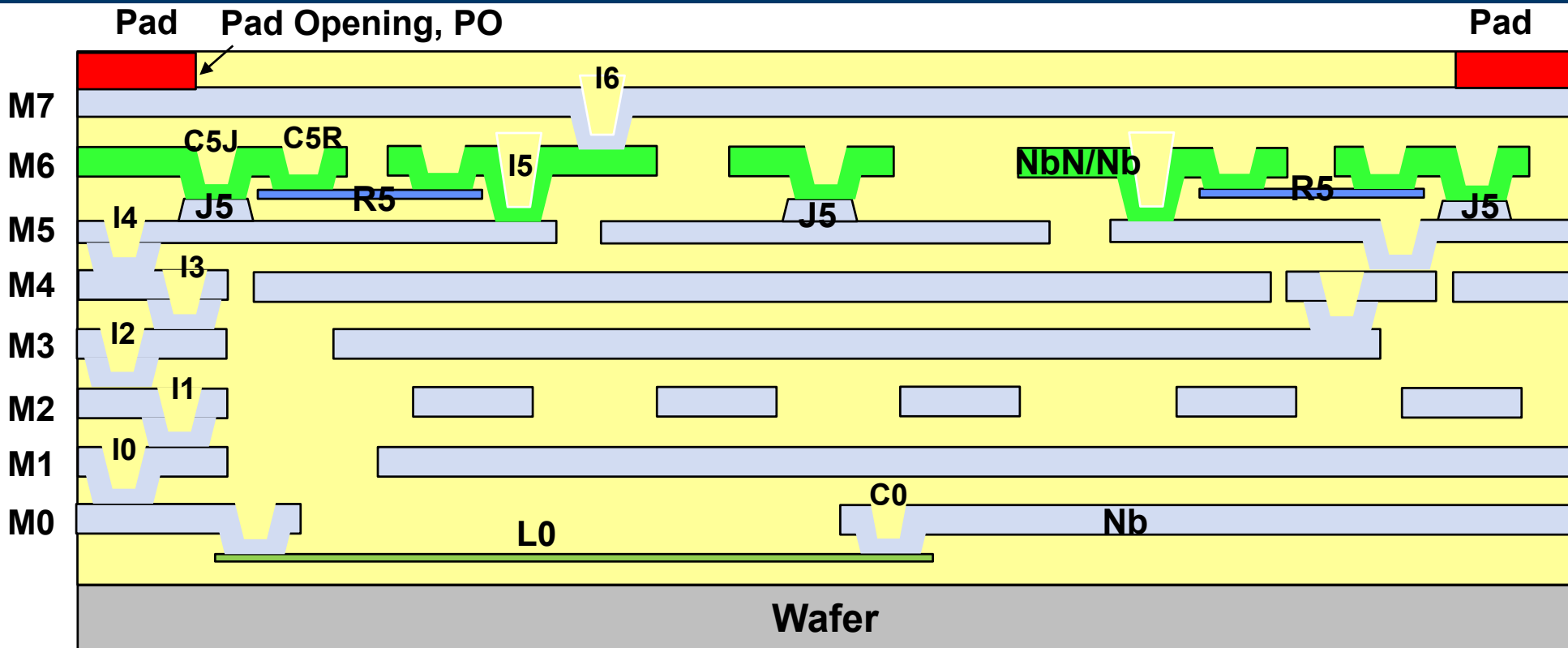
# Outline

- Introduction
- Motivation: why we want NbN layers in the process stack
- Properties of NbN films
  - Critical currents of lines and vias
  - 1-NbN + 7-Nb-layer process SFQ5e++
  - Inductance and mutual inductance of NbN inductors in the 9-metal-layer process ([poster 1EPo2A-8 today](#))
- Why we do not want all NbN layers in the process stack
- Reconciliation of the requirements: Bilayer NbN/Nb inductors; [see also Invited poster 2EPo2F-1 on Tuesday, 2:15 pm – 4:15 pm](#)
- Conclusion

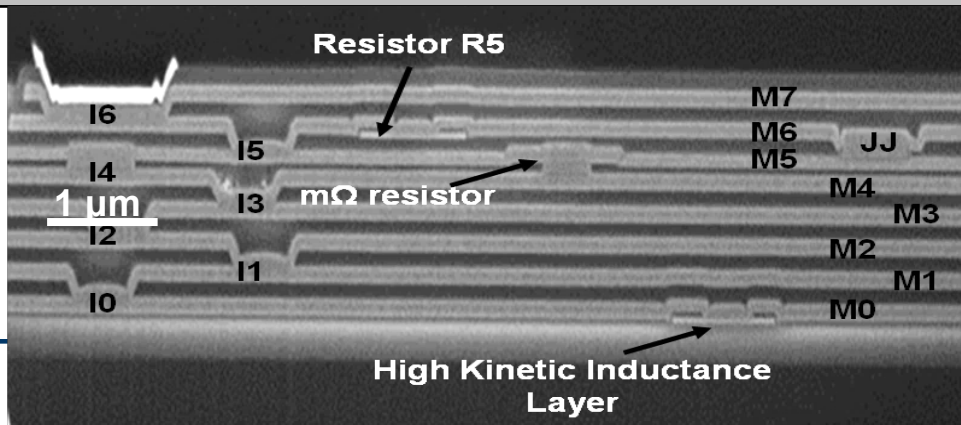




# 1NbN+7Nb-layer Process SFQ5ee++



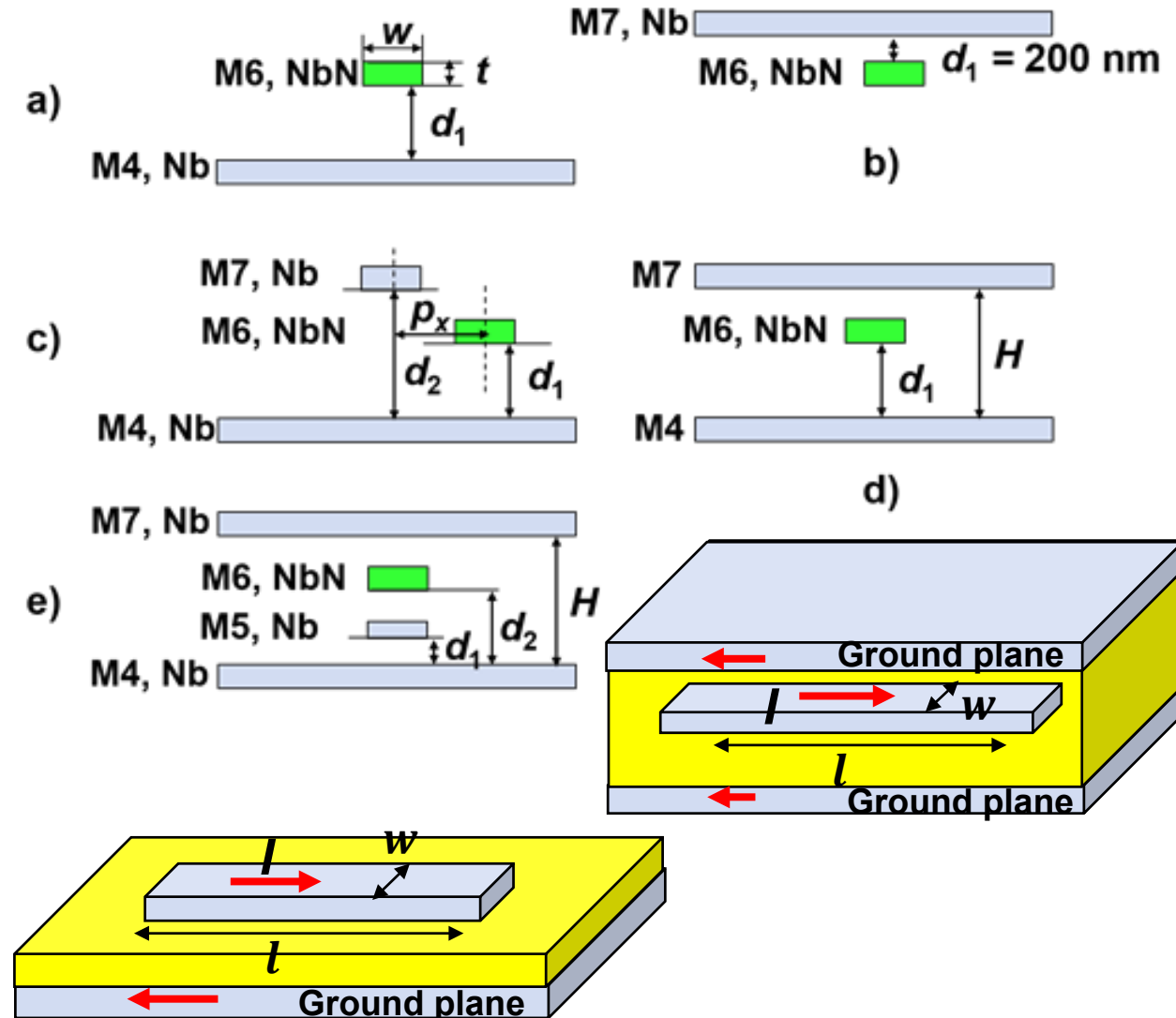
- M6: NbN or NbN/Nb bilayer, 200 nm**
- M0-M4, M7: Nb layers, 200 nm**
- M5: Nb, 150 nm**
- R5: Mo or MoN<sub>x</sub> resistor, 40 nm**
- L0: Mo<sub>2</sub>N kinetic inductor, 40 nm**
- Pad: Nb/Pt/Au**
- I0-I4, I6, I7: vias in SiO<sub>2</sub> interlayer dielectric, 200 nm**
- I5: 270 nm**





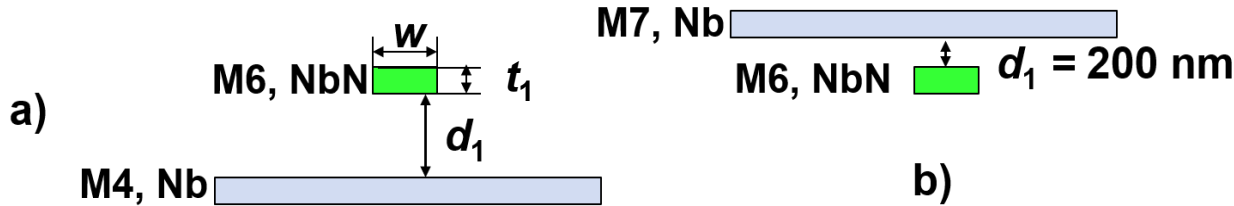
# Self- and Mutual Inductance Structures Measured

- NbN layer with  $T_c \sim 16$  K and 200-nm thickness was incorporated instead of Nb layer M6 in the SFQ5ee process with Nb/Al-AIO<sub>x</sub>/Nb junctions
- Inductance of NbN inductors was measured using SQUID-based integrated circuits for inductance extraction
- Inductors studied:
  - a) microstrips M6aM4
  - b) inverted microstrips M6bM7
  - c) mutual inductance of microstrip inductors M6aM4 and M7aM4;  $p_x$  is distance between geometrical centers of the signal traces in the horizontal, x-direction
  - d) stripline inductors M6aM4bM7
  - e) mutual inductance of striplines M5aM4bM7 and M6aM4bM7;  $p_x$  was varied





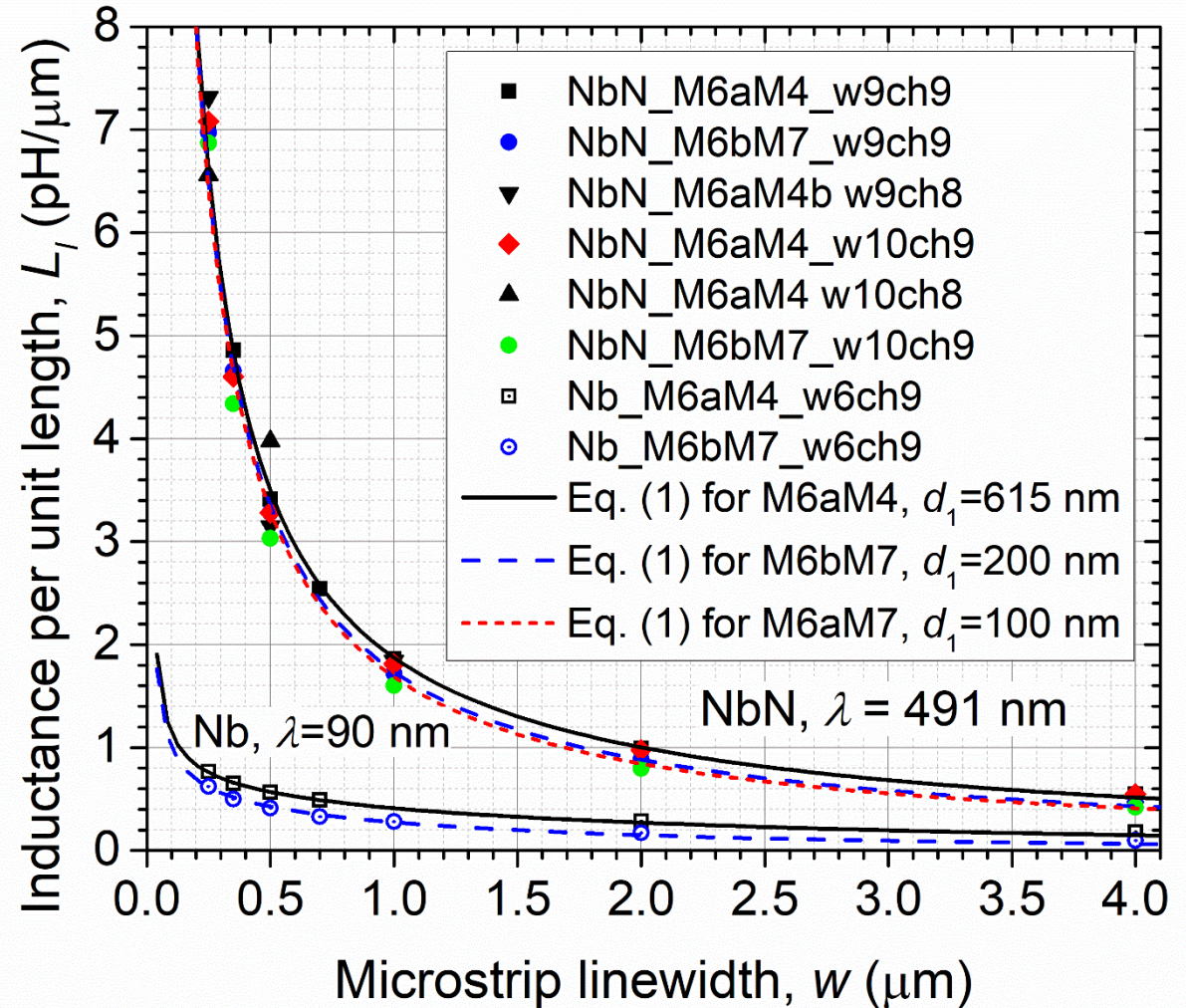
# Inductance of NbN Microstrips with Nb Ground Plane



- Inductance of superconducting microstrips per unit lengths is given by [1]

$$L_l = \frac{\mu\mu_0}{4\pi} \ln \left[ 1 + \frac{4(d_1 + \frac{t_1}{2} + \lambda)^2}{0.2235^2(w + t_1)^2} \right] + \frac{\mu_0\lambda_1^2}{t_1 w}, \quad (1)$$

- Solid and dash curves are fits to (1), giving **magnetic field penetration depth in NbN  $\lambda = 491 \pm 5$  nm** at magnetic field penetration depth in Nb ground planes of  $\lambda = 90$  nm; see the two bottom curves for Nb
- Short dash magenta curve is also a fit to (1) but at a different dielectric thickness  $d_1 = 100$  nm between the layers M6 and M7 on w10
- NbN kinetic inductance  $L_K = 1.51$  pH/sq**







# Inductance of NbN Striplines with Nb Ground Planes

- Superconducting stripline inductance is given in [1]:

$$L_l = \frac{\mu\mu_0}{4\pi} \ln \left( 1 + \frac{\sin^2 \frac{\pi(d_1 + \frac{t_1}{2} + \lambda)}{H+2\lambda}}{\sinh^2 \frac{\pi r_{eq}}{2(H+2\lambda)}} \right) + \frac{\mu_0}{8\pi} + \frac{\mu_0 \lambda_1^2}{t_1 w}, \quad (2)$$

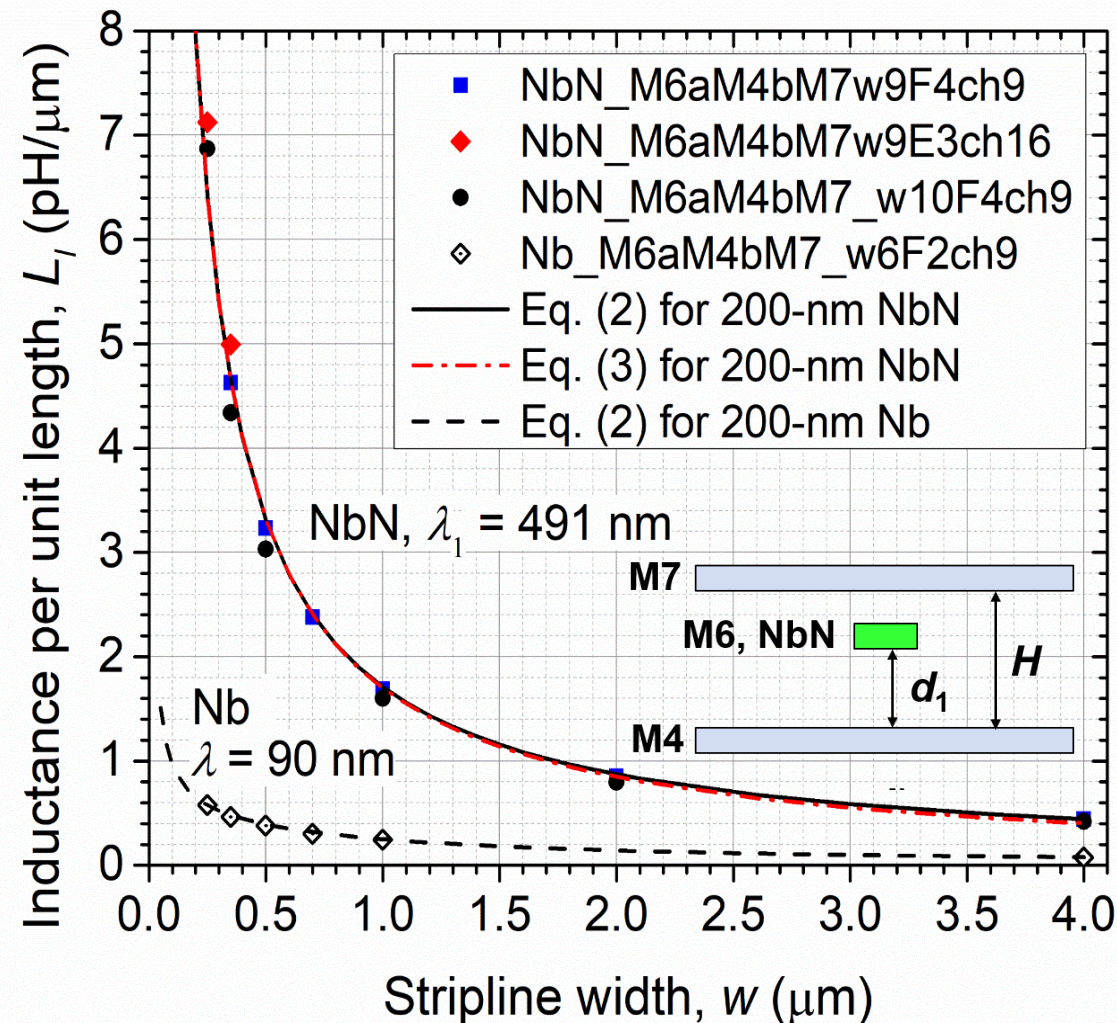
where  $r_{eq}$  is the equivalent radius of the rectangular cross section

- Stripline inductance can also be obtained using Maxwell's geometric mean distance method, calculating self-inductance as mutual inductance of the rectangular wire with itself placed at the geometrical mean distance:

$$L_l = \frac{\mu\mu_0}{4\pi} \ln \left( 1 + \frac{\sin^2 \frac{\pi(d_1 + \frac{t_1}{2} + \lambda)}{H+2\lambda}}{\sinh^2 \frac{0.2235\pi(w+t)}{2(H+2\lambda)}} \right) + \frac{\mu_0 \lambda_1^2}{t_1 w}, \quad (3)$$

where  $0.2235(w+t_1)$  is Maxwell's geometrical mean distance for a rectangular cross section

- NbN kinetic inductance:  $L_k = 1.51 \text{ pH/sq}$







# Mutual Inductance of NbN and Nb Microstrips

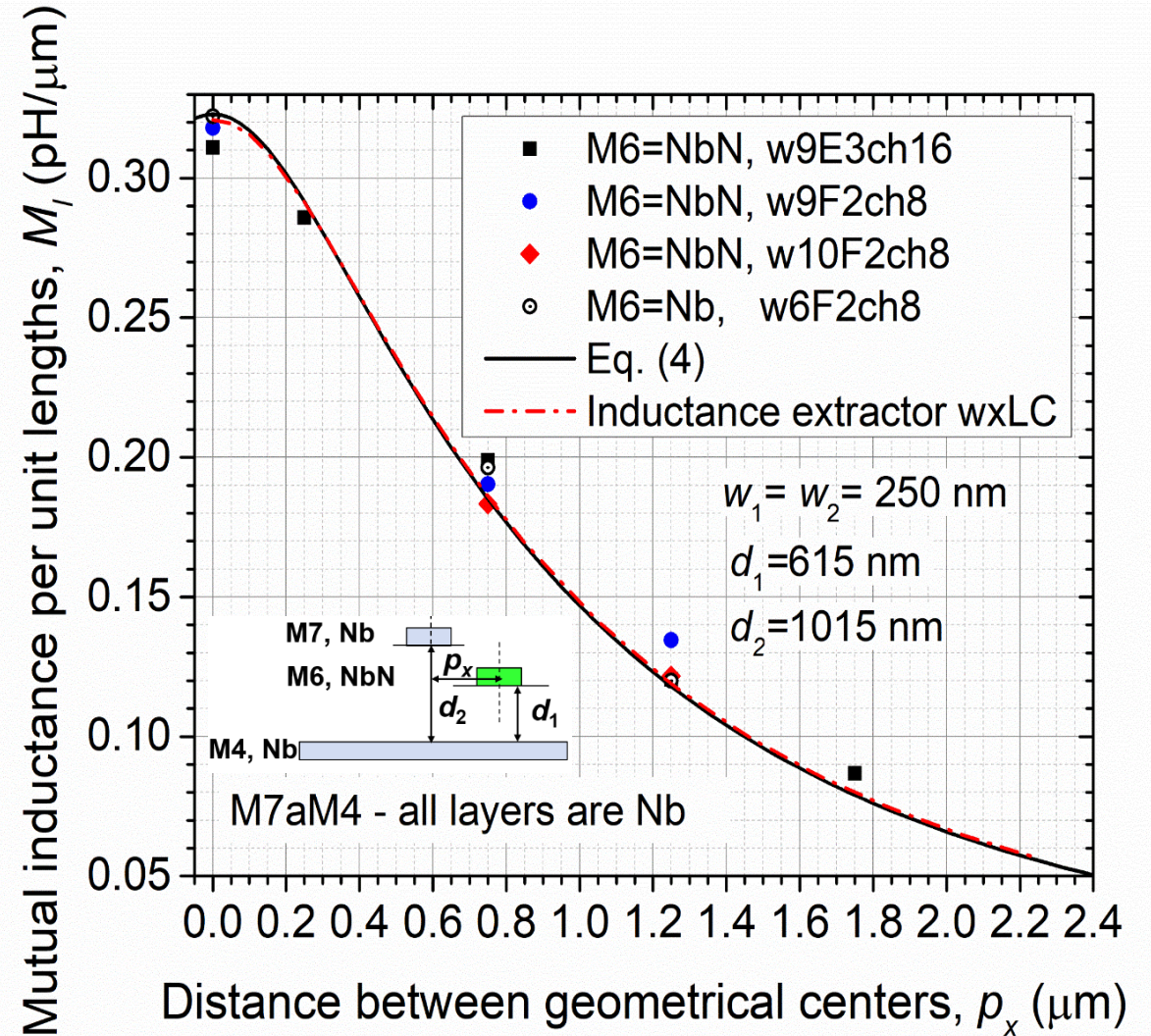
- Mutual inductance of two superconducting microstrips with thicknesses  $t_1$  and  $t_2$ , dielectric thicknesses  $d_1$  and  $d_2$ , and linewidths  $w_1, w_2 \approx |d_2 - d_1|$  is given in [1] by

$$M_l = \frac{\mu\mu_0}{4\pi} \ln \left[ 1 + \frac{4(d_1 + \lambda + \frac{t_1}{2}) \cdot (d_2 + \lambda + \frac{t_2}{2})}{p_x^2 + (d_2 - d_1 + \frac{t_2 - t_1}{2})^2} \right] \quad (4)$$

- Mutual inductance per unit length between NbN and Nb microstrips is the same as between two Nb microstrips (open dots in the Figure)
- Solid black curve is (4) at magnetic field penetration depth in the Nb ground plane  $\lambda = 90$  nm and  $d_1 = 615$  nm, and  $d_2 = 1015$  nm. Red dash-dot curve shows numerical simulation using inductance extractor wxLC
- However, mutual coupling constant

$$\kappa = \frac{M_{12}}{(L_1 L_2)^{1/2}}$$

diminishes with increasing kinetic inductance





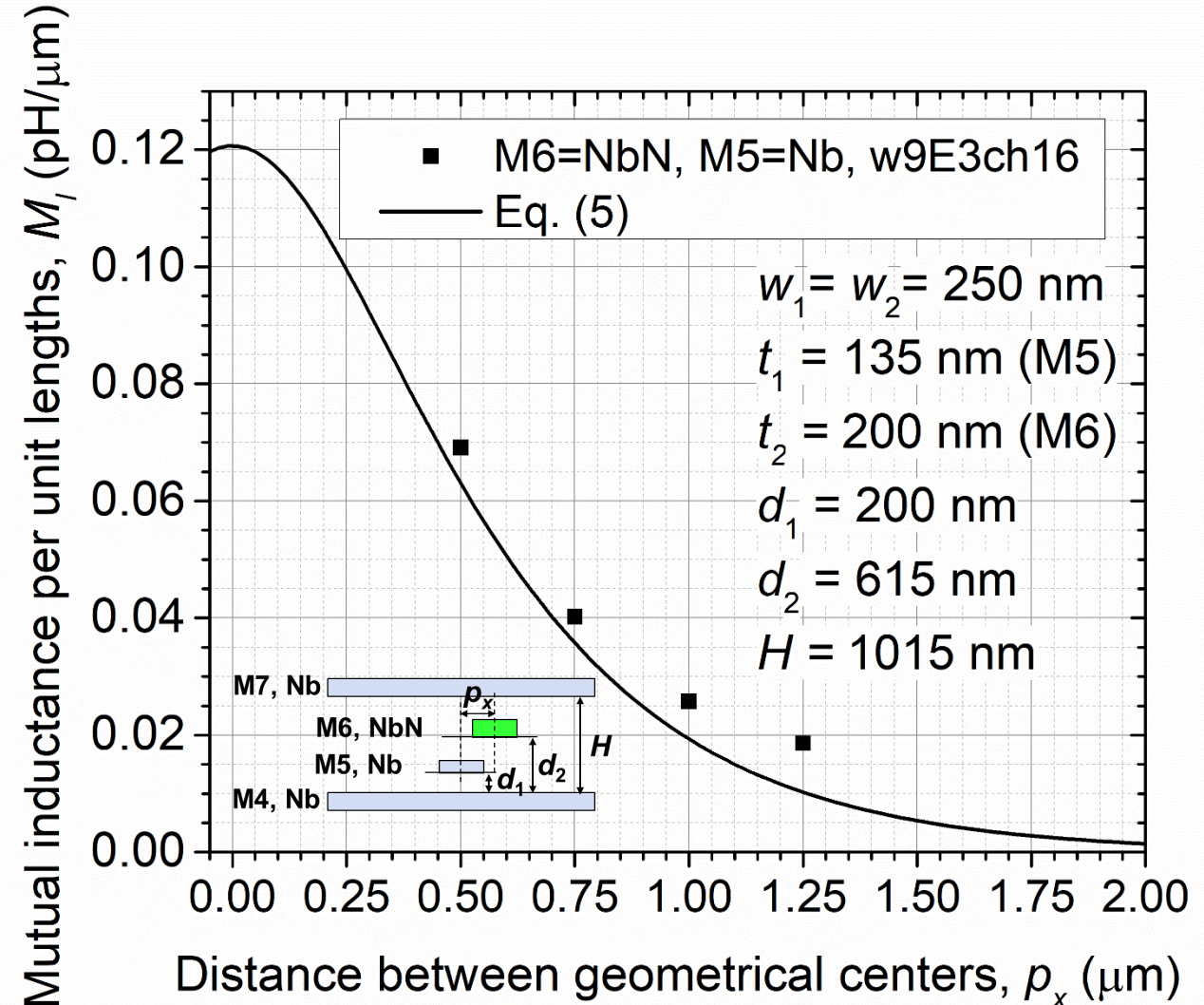


# Mutual Inductance of NbN and Nb Striplines

- Mutual inductance of two superconducting striplines with thicknesses  $t_1$  and  $t_2$ , dielectric thicknesses  $d_1$  and  $d_2$ , and linewidths  $w_1, w_2 \approx |d_2 - d_1|$  is given in [1] by

$$M_l = \frac{\mu\mu_0}{4\pi} \ln \frac{\cosh \frac{\pi p_x}{H+2\lambda} - \cos \frac{\pi(d_1+d_2+t_1+t_2+2\lambda)}{H+2\lambda}}{\cosh \frac{\pi p_x}{H+2\lambda} - \cos \frac{\pi(d_2-d_1+t_2-t_1)}{H+2\lambda}} \quad (5)$$

- Mutual inductance of NbN and Nb striplines is the same as between Nb striplines
- However, the coupling constant  $\kappa = \frac{M_{12}}{(L_1 L_2)^{1/2}}$  diminishes because of kinetic inductance





# Why We Do Not Want Only NbN Layers in the Stack

- High penetration depth  $>0.3 \mu\text{m}$  makes NbN and NbTiN unsuitable for circuit ground (sky) planes:
  - Very poor interlayer shielding
  - Very high parasitic mutual inductance (intralayer coupling) between inductors and logic cells
  - To provide the same shielding as Nb, thickness of NbN ground plane layers should be  $\sim 1.1 \mu\text{m}$
- High kinetic inductance decreases length (and area) of inductors – Good for circuit density
- However, short inductors have low mutual inductance – Good for reducing parasitic crosstalk. Bad for AC power and flux bias transformers
- Kinetic inductors are not suitable for ac power and data PTLs
  - Make PTL impedance too high,  $Z = (L/C)^{1/2}$
  - At the same linewidth,  $Z$  of PTLs with NbN signal traces is 3x higher than  $Z$  of Nb PTLs
  - Or need 3x wider PTLs
- Inductance of vias filled by NbN is  $\gg$  of Nb vias and no longer negligible
- Therefore, we need a right mix of NbN and Nb layers: Nb for ground planes, PTLs, and transformers; NbN for cell inductors



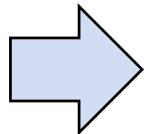


# Outline

**“It makes no good to point out the failures without showing at the same time the remedy to address them”**

**Johann Wolfgang von Goethe**

- **Introduction**
- **Motivation for using NbN in the process stack**
- **Properties of NbN films**
  - **Critical currents of lines and vias**
  - **1-NbN + 7-Nb-layer process SFQ5e++**
  - **Inductance and mutual inductance of NbN inductors in the 9-metal process layer stack**
- **Why we do not want all NbN layers in the process stack**
- **Reconciliation of the requirements: Bilayer NbN/Nb inductors**
- **Conclusion**

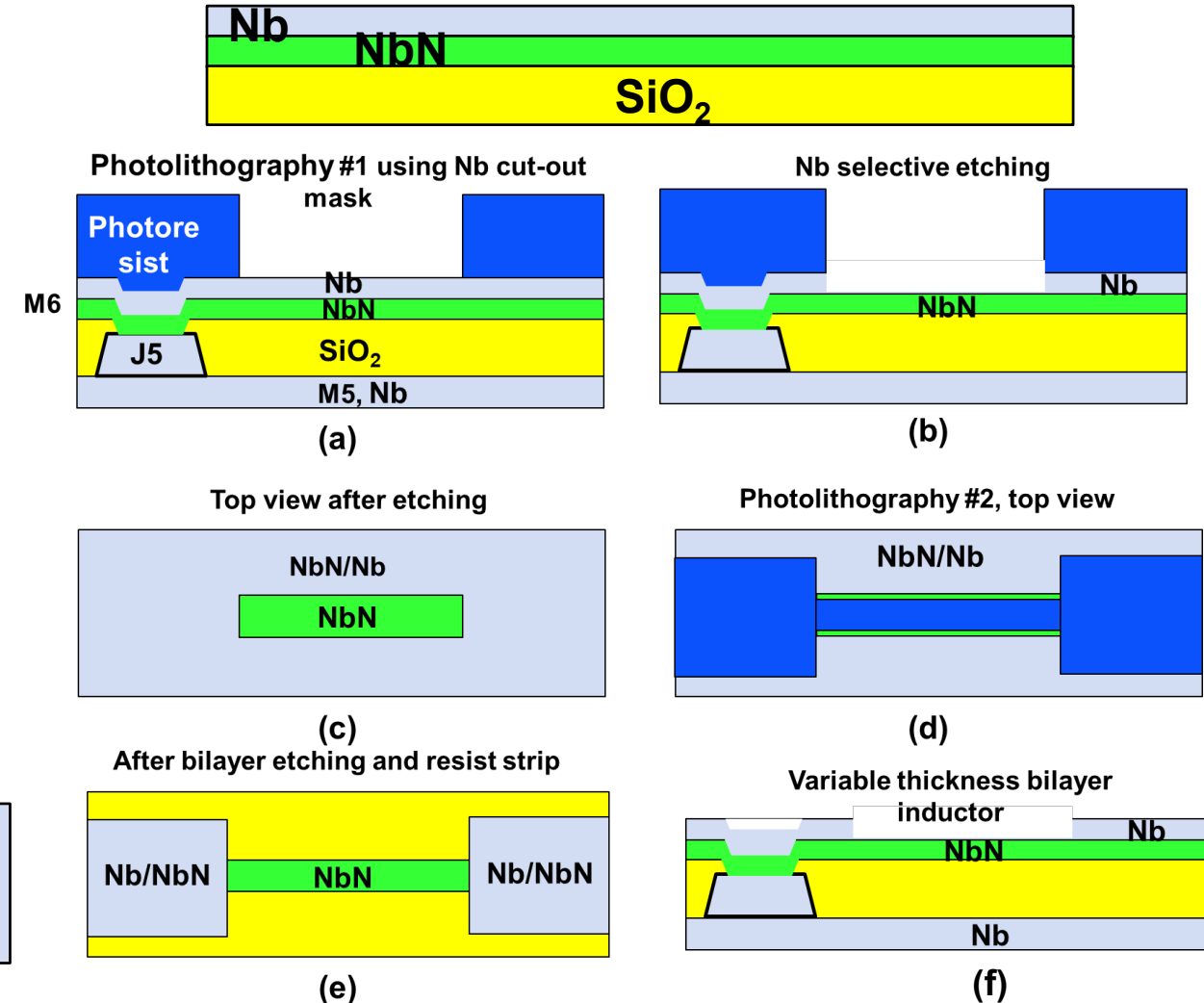




# Reconciliation: Bilayer NbN/Nb Inductors and Transformers

- We have developed and implemented bilayers of magnetic (geometrical) inductors on top of kinetic inductors: NbN/Nb bilayers with 100 nm /100 nm thicknesses (variable process / circuit-design-informed parameter)
  - Since  $\lambda_{NbN} \gg \lambda_{Nb}$ , bilayer inductance is the same as of 100-nm Nb layer – can be used for low-inductance interconnects, PTLs, vias, etc.
  - Mutual inductance of 200-nm-thick bilayer strips is the same as of 200-nm Nb strips – can be used for transformers
  - Selective patterning of the top Nb layer opens access to the bottom NbN kinetic inductance layer
  - Using two photolithography steps and two etch steps (two-step patterning) creates variable thickness and variable (if needed) width inductors
- Gigantic inductance range: from 0.3 pH/μm (like Nb geometrical inductors) to ~ 30 pH/μm (like NbN kinetic inductors)

## NbN/Nb bilayers as inductor layers





# Conclusion

- **We have developed conformal deposition and CMP of superconducting NbN using PECVD from metalorganic precursors for damascence processing of vias and narrow trenches**
- **We incorporated NbN layer and NbN/Nb bilayer into the full layer stack with Nb layers as a dedicated inductor layer**
- **Self- and mutual inductance of NbN inductors with Nb ground planes was studied to provide input data for circuit design**
- **Magnetic field penetration depth in 200-nm thick NbN films deposited by reactive sputtering was determined to be  $491 \pm 5$  nm at 4.2 K, giving kinetic inductance of 1.51 pH/sq**
- **Mutual inductance between NbN and Nb, between NbN and NbN microstrips and striplines was found to be the same as for Nb structures with the same geometrical dimensions and placement between the ground plane, as predicted**
- **Implementation of kinetic inductors in logic (and memory) cells allows for a 10x increase in the integration scale (device number density) of SCE**
- **We welcome suggestions from the community on other useful features to incorporate in the next node of our fabrication process**



# Thank you very much for your attention

## Questions?

**“If you want a wise answer, ask a reasonable question”**

**– Johann Wolfgang von Goethe**